Ultrasensitive Surface Spectroscopy with a Miniature Optical Resonator

Andrew C. R. Pipino*

Process Measurements Division, Chemical Science and Technology Laboratory, National Institute of Standards and Technology, 100 Bureau Drive, Gaithersburg, Maryland 20899-8363

(Received 18 June 1999)

The number density and orientation of molecules at the surface of a total-internal-reflection-ring minicavity are probed with extremely high sensitivity in a novel realization of the cavity ring-down optical absorption experiment. The modes of the ultralow-loss cavity, which are excited by photon tunneling, have long lifetimes that are sensitive to the presence of absorbing species in the evanescent field near a cavity facet. The total-internal-reflection-ring cavity extends cavity ring-down spectroscopy to surfaces and condensed matter, permitting a wide range of novel fundamental studies and applications. Routine single molecule detection may ultimately be feasible.

PACS numbers: 82.65.Pa, 42.79.–e, 78.20.–e, 82.80.Ch

In recent years, the use of an optical cavity to enhance sensitivity in absorption spectroscopy has shown considerable promise [1], with the potential for reaching the shot-noise detection limit at high fluence [2,3]. Cavity ring-down spectroscopy (CRDS) [4–6] is one particularly prevalent implementation of cavity enhanced absorption spectroscopy for gases in which photon lifetime in a low-loss cavity is the absorption-sensitive observable. However, CRDS has remained essentially a gas phase spectroscopic method due to the large intrinsic loss introduced by most condensed matter sampling schemes and the narrow spectral bandwidth of ultrahigh reflectivity mirrors, although some progress has been made [7,8]. Given the fundamental importance of optical absorption measurements, extension of CRDS to other states of matter has substantial potential for impact in the physical, chemical, and biological sciences. This Letter describes a novel strategy that comprehensively extends CRDS to surfaces and condensed matter by employing a monolithic, total-internal-reflection(TIR)-ring minicavity [9,10].

The principles and applications of CRDS have been reviewed elsewhere [5,6]. Briefly, in a typical gas-phase CRDS experiment, a stable optical cavity is formed from a pair of concave, highly reflective mirrors. When a light pulse, usually from a laser source, is injected into the cavity, the circulating intensity decays exponentially with a frequency-dependent "ring-down" time, $\tau(\omega)$, given by the ratio of the round-trip time, t_r, to the sum of the round-trip losses, or

$$\tau(\omega) = \frac{t_r}{L_0(\omega) + L_{\mathrm{abs}}(\omega)}, \qquad (1)$$

where $L_0(\omega)$ is the intrinsic cavity loss, and $L_{\mathrm{abs}}(\omega)$ arises from absorption by gases contained within the cavity. The difference in intensity decay rates for the gas-filled and empty cavities as a function of laser frequency provides the absolute absorption spectrum of the sample. Since the intensity decay rate ($\propto 1/\tau$) is employed instead of a ratio of intensities, as in conventional absorption spectroscopy, the measurement is essentially immune to noise introduced by light source fluctuations. The minimum detectable absorption in CRDS can be expressed as the product of the relative uncertainty in the ring-down time and the intrinsic cavity loss [11], or $\alpha_{\mathrm{min}} = (\Delta\tau/\tau)_{\mathrm{min}} {}^{*} L_0$. This form for α_{min} reveals the simplicity and challenge of CRDS: Minimize the intrinsic cavity loss and determine the ring-down time with the highest possible precision.

To extend CRDS to surfaces and condensed matter, the properties of TIR are employed. For a plane wave incident on a perfectly smooth interface between two media with indices of refraction n_1 and n_2, TIR occurs when the angle of incidence θ_i exceeds the critical angle, defined by $\theta_c = \sin^{-1}(n_2/n_1)$, which in theory provides a perfect ($R = 1$), broadband mirror. In practice, the reflectivity is less than unity due to surface roughness scattering and nonspecular transmission arising from the nonplanar character of real wave fronts. Yet ultrasmooth polished surfaces with root-mean-square surface roughness of $\sim$0.05 nm can be generated routinely for many optical materials, yielding effective mirror reflectivities of $R \sim 0.999\,999$ in the visible region of the spectrum. Furthermore, TIR generates an evanescent wave with a locally enhanced surface electric field at the TIR interface, which permits absorption of an ambient medium to be probed as in the well-known technique of attenuated total reflectance [12]. A general applicability to surfaces is achieved because the TIR condition is not perturbed by the presence of a film that is thin relative to the evanescent wave decay length, but sufficiently thick to achieve the chemical equivalence of a semi-infinite surface. Even for strongly absorbing media, a sparse distribution of islands, clusters, or adatoms, can be used to provide insight into fundamental chemical interactions. To fully exploit the properties of TIR for CRDS, a TIR-ring cavity is required.

In Fig. 1, a square, TIR-ring cavity is depicted with a single, convex facet that is required to form a stable optical resonator. In general, the angle of incidence for a regular, polygonal TIR-ring cavity with n facets is given by $\theta_i = \pi(n - 2)/2n$. For a judicious choice of n, $\theta_i > \theta_c$ is fulfilled by the single θ_i for the full transmission range of a

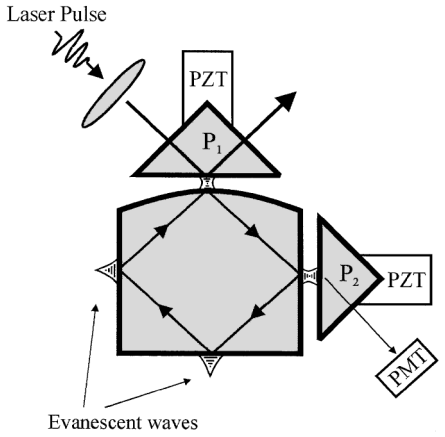

FIG. 1. A total-internal-reflection-ring minicavity is depicted that achieves a comprehensive extension of CRDS to surfaces and condensed matter. The cavity is fabricated from ultrahigh-transmission optical material in the form of a regular polygon with a convex facet that refocuses the internally circulating light, forming a stable optical resonator. Light enters and exits the ring by photon tunneling through coupling prisms, P_1 and P_2. The extremely small round-trip optical loss results in long ring-down times, which are highly sensitive to the presence of an absorbing medium in the evanescent fields emanating from the remaining facets.

given optical material, providing broad spectral bandwidth. The square geometry forms the simplest fused-silica resonator that sustains modes by TIR from the ultraviolet to the near-infrared region. Photon tunneling across the junctions between the monolithic cavity and the coupling prisms P_1 and P_2 is used to excite and monitor the modes, respectively, since direct excitation of a cavity mode by a propagating wave is forbidden. The dependence of coupling efficiency, cavity finesse, and resonance frequency on the tunneling junction has been investigated previously by Schiller *et al.* [13] for a low-finesse resonator. At the impedance-matched condition where the round-trip loss equals the coupling loss, the on-resonance transmission is near unity. At larger gap widths, the finesse approaches a constant, maximum value, where coupling losses are small relative to other losses. Operation in the weakly coupled region therefore maximizes and stabilizes the ring-down time with respect to variations of the tunneling junction. Evanescent waves emanate from the remaining facets to probe the absorption of an ambient medium.

The relationship between the ring-down time and sample absorption for the TIR-ring cavity is described by Eq. (1) with $L_0(\omega) = L_{\text{bulk}} + L_{\text{diff}} + L_{\text{surf}} + L_{\text{nspec}} + L_{\text{coup}}$, where L_i correspond to bulk, diffraction, surface scattering, nonspecular, and coupling losses, respectively. The magnitude and frequency dependence of the different losses have been examined in detail previously [9]. With proper material selection and cavity design, $L_0(\omega)$ can be in the range of $1 \times 10^{-7} \leq L_0 \leq 1 \times 10^{-3}$ over broad spectral regions, yielding long ring-down times that can be measured with high precision.

The initial experiments used a 7.5 mm $\times$ 7.5 mm $\times$ 5.0 mm square cavity which was fabricated from selected fused silica. The cavity facets, including a 2.23 cm radius of curvature convex facet, were polished to 0.05 nm rms surface roughness. As indicated in Fig. 1, piezoelectric translators were used to provide precise (± 5 nm) control of the tunneling junctions. Simple interferometry permitted absolute measurement and monitoring of the junctions. With diffraction, surface scattering, and nonspecular losses rendered small by design and fabrication, the intrinsic cavity loss becomes bulk-loss limited if weak coupling is employed. Figure 2 shows the round-trip intrinsic loss and ring-down time on opposite axes as a function of wavelength for the square cavity. Each data point was obtained by averaging 75 ring-down times which were extracted from single-shot decays by using a weighted fitting routine. An excimer-pumped, pulsed dye laser, which generated 20 ns, $\sim$1 mJ pulses, was used as the excitation source without mode matching. The decay waveforms were detected with a photomultiplier tube and an eight-bit digital oscilloscope, as in Ref. [7]. Over the wavelength region of Fig. 2, the intrinsic loss decreases rapidly, corresponding to the decreasing bulk loss for fused silica. At 580 nm, $L_0 = 80 \times 10^{-6}$, which yields a minimum detectable absorption of $\alpha_{\text{min}} \leq 1.6 \times 10^{-7}$, given a relative uncertainty in the decay time of 0.2% or better. Above 600 nm, the bulk losses of fused silica decrease substantially, reaching a minimum of $\sim 5 \times 10^{-7}$ cm^{-1} in the near-IR. Extremely high sensitivity absorption measurements can be anticipated in this spectral region, possibly reaching single molecule detection as discussed below. Yet, even at 450 nm, a ring-down of $\sim$200 ns for this cavity remains sufficiently long to permit absorptions of $\sim 1 \times 10^{-6}$ to be detected. Furthermore, since both in-plane (p) and out-of-plane (s) polarizations have high finesse for the TIR-ring

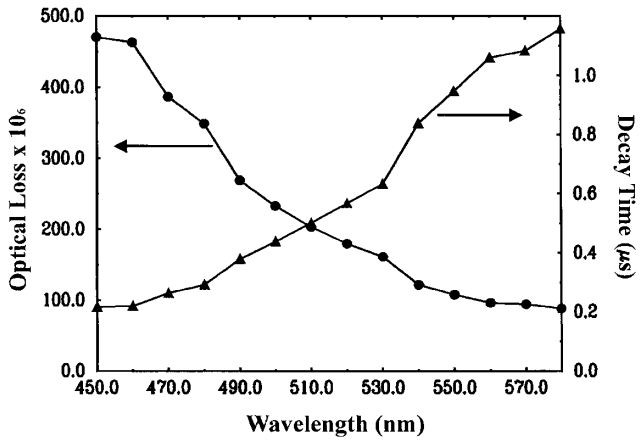

FIG. 2. The round-trip intrinsic loss (in parts per million) and ring-down time (in microseconds) are shown on opposite axes as a function of wavelength for a fused-silica cavity, as in Fig. 1, with a 2.12 cm round-trip path length and a 2.23 cm radius-of-curvature convex facet.

cavity, a rich variety of polarization dependent phenomena can be probed.

Figure 3 shows single-shot ring-down traces with decay times of 1.270 and 1.278 μs for s- and p-polarized cavity modes, respectively, obtained at 580 nm for the nascent resonator. The inset of Fig. 3 defines the surface coordinate system and shows the components of the electric field intensity of the evanescent wave as a function of distance from the cavity facet [12]. An understanding of the direction and magnitude of the electric field intensity is essential for interpreting optical absorption by a surface-bound molecule, since only an optical field component that is parallel to the molecular transition dipole moment will be absorbed. At the TIR surface ($z = 0$), the x, y, and z components of the field intensity, $|E_x|^2$, $|E_y|^2$, and $|E_z|^2$, are modified by factors of 0.4112, 3.783, and 7.154, respectively, relative to the incident field intensity. The p-polarized cavity mode, which is composed of E_x and E_z, is dominated by the strongly enhanced z component that is normal to the cavity facet, while the s mode is composed of E_y only, which lies in the plane of the TIR surface. With knowledge of the field magnitude and direction, measurement of the dichroic ratio of s- to p-polarized absorptions, $\rho = A_s/A_p$, can be related to the molecular orientation [14]. Figure 4 shows ring-down traces for s- and p-polarized modes under identical conditions with Fig. 3, but a TIR facet has been exposed to I_2 vapor [15], which has a visible $X \leftarrow B$ transition dipole moment that is aligned with the molecular axis. The inset of Fig. 4 shows the polar and azimuthal angles, θ and ϕ, respectively, for describing orientation of adsorbed iodine. Note that both s- and p-polarized modes show a change in ring-down time with $\tau_s = 0.497$ μs and $\tau_p = 0.889$ μs, but the s-polarized mode shows a significantly larger change, despite the smaller field enhancement associated with E_y, suggesting that I_2 molecules are preferentially oriented with their molecular axes parallel to the surface.

To describe orientation quantitatively, a distribution function $N(\theta, \phi)$ should be invoked. A common strategy is to expand $N(\theta, \phi)$ in spherical harmonics, reducing the measurement to a determination of expansion coefficients d_{lm}. In general, dichroic ratio measurements yield only the value of d_{20}, which is often referred to as the "order parameter." $N(\theta, \phi)$ is frequently assumed to be isotropic in φ and sharply peaked in θ, leading to the interpretation of d_{20} in terms of an average polar angle θ_{avg}, obtained from $d_{20} = (3\cos^2\theta_{\text{avg}} - 1)/2$. From the results of Figs. 2 and 3, $d_{20} = -0.50$ is found, which yields $\theta_{\text{avg}} = 90°$, corroborating the conclusion that I_2 lies flat on the resonator surface. Yet at a given precision for d_{20}, many distribution functions are possible, differing in shape, width, and most probable angle. By improving the precision of d_{20} measurements, some differentiation between distributions may be possible [16]. The greater sensitivity provided by the TIR-ring cavity will enable more precise dichroic ratio measurements for weakly

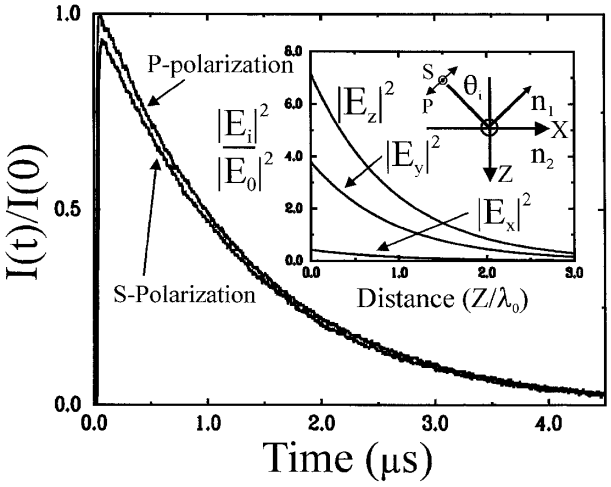

FIG. 3. Ring-down traces for s- and p-polarized modes of a fused-silica, square-TIR-ring minicavity are shown for a single laser pulse at 580 nm, where the s-polarized decay is slightly offset for presentation purposes. The cavity modes incur a fractional loss of only $\sim 80 \times 10^{-6}$ per round-trip. The inset shows the electric field intensity components of the evanescent wave calculated using the Fresnel equations as a function of distance from a cavity facet relative to the incident intensity. The surface coordinate system is also shown. Knowledge of surface field direction and magnitude allows molecular orientation to be probed for an absorbing molecule at the surface.

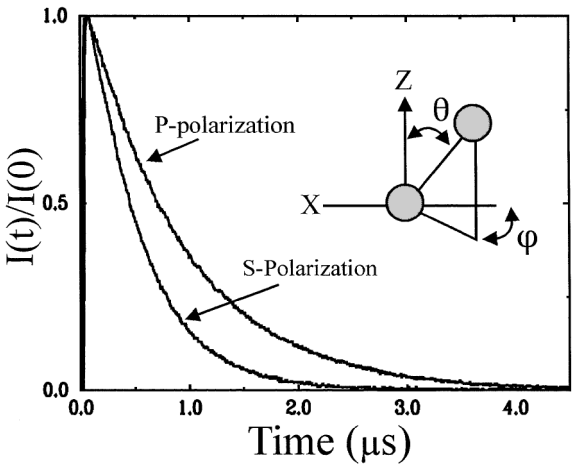

FIG. 4. Ring-down traces for s- and p-polarized modes for the identical conditions of Fig. 3, but a TIR facet of the resonator has been exposed to I_2 vapor at ambient temperature. Optical absorption by molecules in the evanescent field of a cavity facet is detected as a decrease in the ring-down time arising from an increase in the round-trip loss. Both polarizations show a change in decay time, but a larger change for the s-polarized mode suggests that I_2 molecules lie flat on the surface, since the electric field for this mode is parallel to the surface. The inset shows the relevant angular coordinates for describing orientation. The base ring-down time of Fig. 2 is regained with removal of the I_2 source.

absorbing systems, potentially providing more decisive measurements of orientation.

In addition to providing insight into surface bonding and reactivity, knowledge of molecular orientation is also required to quantify of surface coverage, which has been a long-standing problem in surface science. The absorption cross section for the surface-bound species is also required, but is generally not known. In addition, chemically different surface sites and surface chemical reactions can occur and are likely important on the nascent SiO_2 surface of the resonator. Iodine serves as a suitable probe molecule because the gas-phase peak absorption cross section at 520 nm of 2.56×10^{-18} cm^2/molecule [17] does not change substantially with physisorption [18]. Assuming I_2 is physisorbed and lies flat on the surface, an estimated minimum detectable coverage of $\sim$0.006% of a monolayer (1 monolayer $= 4.5 \times 10^{14}$ sites/cm^2) is obtained. This estimate is based on a minimum detectable absorption of 1.9×10^{-7}, which is achieved for a 25 laser shot average, providing a relative standard deviation in τ of 0.2% (instrumentation-limited). Significant improvements in sensitivity can be anticipated by reaching the shot-noise limit at high fluence and by further reducing intrinsic loss.

To obtain the highest sensitivity, excitation of only the lowest order transverse cavity mode, TEM_{00}, must be employed, which significantly improves decay time precision [2]. Single transverse mode excitation is facilitated by the use of a narrow linewidth source, which also results in increased light throughput as the laser linewidth approaches the cavity linewidth. Since the shot-noise-limited uncertainty is $N^{-1/2}$, where N is the number of photons arriving at the detector, the uncertainty improves with increasing throughput. By achieving shot-noise-limited detection at high fluence, the ultimate sensitivity will be achieved. Sensitivity will also increase when working in other spectral regions, by employing other optical materials with lower bulk attenuation, or by reducing the size of the resonator to its optimum value [9]. For example, consider detection of the surface hydroxyl groups of the nascent resonator surface. In the near-IR, a bulk attenuation of $\sim 5 \times 10^{-7}$ cm^{-1} can be obtained for fused silica, which will permit absorptions of $\leq 10^{-10}$ to be measured. Assuming an absorption cross section of $\sim 10^{-18}$ cm^2/molecule, detection of $\sim$600 surface OH groups ($\sim 3 \times 10^{-8}$ of a monolayer) in the 31 μm $\times$ 44 μm elliptical area sampled by a resonator as in Fig. 1 should be feasible. Different forms of the surface hydroxyl group, such as vicinal or terminal SiOH or adsorbed water, can also be spectrally distinguished to probe the surface chemistry of this technologically important system. At this sensitivity level, density fluctuations should be detectable, which are precursory to single molecule detection [19]. In the mid-IR, where vibrational spectroscopy is most informative, certain fluoride glasses [20] can provide a bulk attenuation of $< 1 \times 10^{-7}$ cm^{-1}, which should permit single molecule detection of a wide variety of chemical species, possibly at ambient temperature.

This work was supported by the Environmental Management Science Program of the Department of Energy under Contract No. DE-AI07-97ER62518.

*Email address: andrew.pipino@NIST.gov

[1] J. Ye, L.-S. Ma, and J. L. Hall, J. Opt. Soc. Am. B **15**, 6 (1998).
[2] R. D. van Zee, J. T. Hodges, and J. P. Looney, Appl. Opt. **38**, 3951 (1999).
[3] M. D. Levenson *et al.*, Chem. Phys. Lett. **290**, 335 (1998).
[4] A. O'Keefe and D. A. G. Deacon, Rev. Sci. Instrum. **59**, 2544 (1988).
[5] M. D. Wheeler, S. M. Newman, A. J. Orr-Ewing, and M. N. R. Ashfold, J. Chem. Soc. Faraday Trans. **94**, 337 (1998).
[6] J. J. Scherer, J. B. Paul, A. O'Keefe, and R. J. Saykally, Chem. Rev. **97**, 25 (1997).
[7] A. C. R. Pipino, J. W. Hudgens, and R. E. Huie, Chem. Phys. Lett. **280**, 104 (1997).
[8] R. Engeln, G. von Helden, A. J. A. van Roij, and G. Meijer, J. Chem. Phys. **110**, 2732 (1999).
[9] A. C. R. Pipino, J. W. Hudgens, and R. E. Huie, Rev. Sci. Instrum. **68**, 2978 (1997).
[10] A. C. R. Pipino, in *Advanced Sensors and Monitors for Process Industries and the Environment*, SPIE Proceedings Vol. 3535 (SPIE-International Society for Optical Engineering, Bellingham, WA, 1998).
[11] P. Zalicki and R. N. Zare, J. Chem. Phys. **102**, 2708 (1995).
[12] N. J. Harrick, *Internal Reflection Spectroscopy* (Interscience, New York, 1967).
[13] S. Schiller, I. I. Yu, M. M. Fejer, and R. L. Byer, Opt. Lett. **17**, 378 (1992).
[14] N. L. Thompson, Harden M. McConnell, and Thomas P. Burghardt, Biophys. J. **46**, 739 (1984).
[15] To dose the cavity facet with I_2 vapor, a 2 mm O.D. glass tube was packed with solid I_2 and inserted in a 5 mm O.D. $\times$ 3 mm I.D. glass tube. The concentric tubes were sealed at one end by a ground-glass joint. An O-ring groove containing a small Viton O-ring was milled into the other end of the 5 mm O.D. tube. The O-ring groove surface was polished to half-wave flatness, allowing interferometry to be used to parallelize the tube end relative to a flat cavity facet. Light contact then provided a vapor-tight seal.
[16] C.-P. Lafrance, A. Nabet, R. E. Prud'homme, and M. Pézolet, Can. J. Chem. **73**, 1497 (1995).
[17] J. G. Calvert and J. N. Pitts, Jr., *Photochemistry* (Wiley, New York, 1967).
[18] G. Kortum and H. Koffer, Ber. Bunsen-Ges. Phys. Chem. **67**, 67 (1963).
[19] *Single-Molecule Optical Detection, Imaging, and Spectroscopy*, edited by T. Basche *et al.* (VCH, Cambridge, 1997).
[20] *Fluoride Glass Fiber Optics*, edited by I. D. Aggarwal and G. Lu (Academic, Boston, 1991).